Physics at a $\gamma\gamma$ Collider

Klaus Mönig

DESY, Platanenallee 6, 15738 Zeuthen, Germany

DOI: http://dx.doi.org/10.3204/DESY-PROC-2009-03/Moenig

A $\gamma\gamma$-collider is a possible extension of an e^+e^- linear collider. The physics case of such a machine will be reviewed and compared to the one of the e^+e^- mode of the machine.

1 Introduction

At a linear collider beams are used only once so that it is possible to "convert" an electron beam into a photon beam by colliding it with an intense laser a few millimetres in front of the interaction point [1, 2, 3]. The high energy photons follow the electron flight direction so that the focusing of the beams works as in the e^+e^- mode. Using one or two lasers the machine can be used as an eγ or $\gamma\gamma$ collider. If the appropriate laser wavelength is chosen the photon beam has an energy of up to 80% of the energy of the incoming electron beam. Figure 1 (left) shows the photon energy spectrum for the different choices of the electron and laser polarisation. To achieve a high peak at maximal energy the helicity of the electron and laser beams must be opposite. Figure 1 (right) shows the resulting beam polarisation for the different cases. The setup that give the best energy spectrum also results in a large and stable polarisation in the high energy peak. Since only the product of the electron and laser polarisation matters the γ-beam polarisation can be varied by flipping both helicities simultaneously and the longitudinal angular momentum of the $\gamma\gamma$ system can be dominantly $J_z = 0$ or $J_z = 2$. In reality the spectrum gets distorted by two effects. To reach a high conversion probability the laser energy must be high which leads to non linear effects distorting the high energy peak. In addition there is a high chance that electrons interact a second time with a laser photon giving rise to a large peak at low energies. The resulting spectrum is shown in Fig. 2 [3].

In addition to circular polarisation also linear polarisation is possible at a photon collider. In this case the laser must be polarised linearly resulting in a less peaked energy spectrum. The linear polarisation in the high energy beam is on the 30% level, the simultaneous circular polarisation around 80%. The luminosity of a photon collider in the high energy part is around 10% of the e^+e^- luminosity for identical beam parameters. Due to the missing beam-beam effects the beams can be squeezed stronger so that a luminosity of $\mathcal{L}_{\gamma\gamma} \approx 0.3\mathcal{L}_{e^+e^-}$ seems possible.

Charged particles at the photon collider are produced via t-channel exchange which leads to a well known cross section proportional to Q^4. Especially for particles with unit charge they are typically one order of magnitude larger than in e^+e^-. Neutral particles like the Higgs can only be produced via loop diagrams, nevertheless the cross sections can be significant.

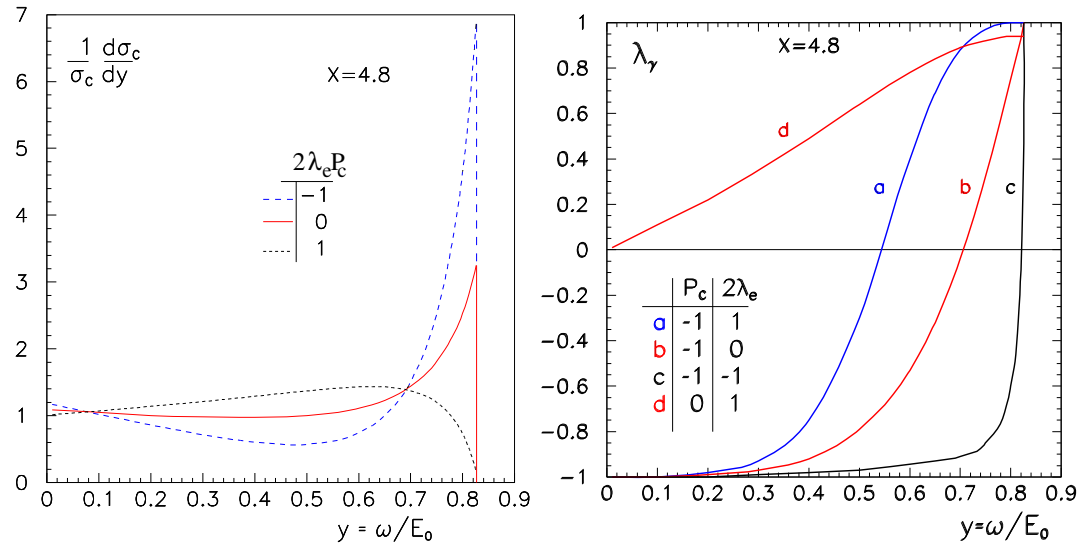

Figure 1: Left: normalised photon energy spectrum from Compton scattering for different electron and laser polarisation; right: photon circular polarisation for different electron and laser polarisation. Because of parity conservation in Compton scattering the missing combinations can be obtained from the shown ones by flipping all involved helicities [2].

2 Higgs Physics

Higgses are produced at the photon collider mainly by the loop graph shown in Fig. 3. All charged particles that couple to the Higgs contribute. In the Standard Model the cross section is dominated by the top-quark and the W-boson and there is a large sensitivity of the production cross section to new heavy charged particles coupling to the Higgs. At the photon collider the Higgs must be identified in a channel with a large branching ratio like $H \to b\bar{b}$ or $H \to W^+W^-$ and the observable $\Gamma(H \to \gamma\gamma) \times BR(H \to X\overline{X})$ is measured. For a light Higgs $BR(H \to b\bar{b})$ can be measured with a precision of around 2% in the e^+e^- mode [5]. For $m_H = 120\,\mathrm{GeV}$ about 10000 events per year will be produced at the photon collider. For Higgs production $J_z = 0$ is needed. For this polarisation state fermion pair production is suppressed by a factor m^2/s so that the background is manageable. Because of the Q^4-dependence of the background cross section a good b-tagging, especially b-c separation, is mandatory.

Detailed MC studies including all experimental and theoretical effects exist [6, 7]. The final mass spectrum is shown in Fig. 4 (left). $\Gamma(H \to \gamma\gamma) \times BR(H \to b\bar{b})$ can be measured with a precision of better than 2%. Combining with the $BR(H \to b\bar{b})$ measurement from the e^+e^- mode [5] this leads to a measurement of the coupling $g_{H\gamma\gamma}$ of around 1.5%.

For a heavier Higgs the decay mode $H \to W^+W^-$ must be used. This mode has the disadvantage of a much larger Standard Model background. However the interference with the $\gamma\gamma \to W^+W^-$ amplitude can also be used to measure the phase of the coupling [8]. The reconstructed WW mass spectrum is shown in Fig. 4 (right). Figure 5 (left) shows the possible precision of $\Gamma(H \to \gamma\gamma)$ as a function on m_H. For relatively light Higgses the precision is similar as in the $b\bar{b}$-mode. Figure 5 (right) shows the predicted change in $\Gamma(H \to \gamma\gamma) \times BR(H \to WW)$

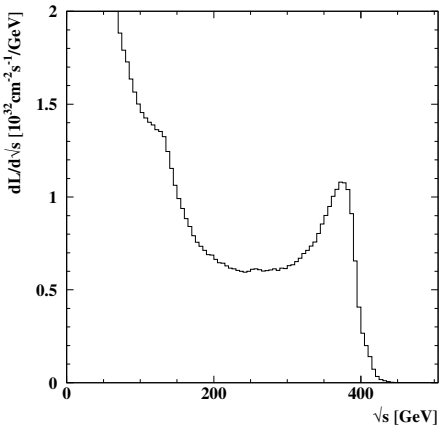

Figure 2: Luminosity spectrum for $\sqrt{s}_{ee} = 500\,\text{GeV}$ including non-linear effects and multiple interactions calculated with CAIN [4].

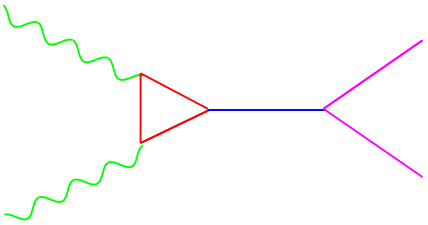

Figure 3: Feynman-graph for Higgs production at the photon collider.

and in the phase of the coupling for a 2HDM model. It can be seen that the phase brings additional information to distinguish the model from the SM or to measure model parameters.

For supersymmetric Higgses the photon collider has a real discovery window. If the A is significantly heavier than the Z the A, H and $H^{\pm}$ are almost mass degenerate and the ZZH and ZZA couplings vanish. The relevant production modes in e^+e^- are thus $e^+e^- \to HA$ and $e^+e^- \to H^+H^-$ and the mass reach is $\sqrt{s}/2$ [5]. For medium $\tan\beta$ and $m_A > 200$GeV also the LHC cannot detect the supersymmetric Higgses [9]. At the photon collider the loop induced s-channel production still works and the mass reach remains $0.8\sqrt{s}_{ee}$. Detailed studies show that the H and A can be reconstructed (see Fig. 6, left) and that it can bee identified with 5σ in at most two years of running (Fig. 6, right) [10].

Another possibility at the linear collider is the use of linear beam polarisation. With a linearly polarised laser a linear beam polarisation of around 30% can be achieved. As can be seen from Fig. 1 this leads, however, to s smaller circular polarisation and a less peaked energy spectrum. With linear beam polarisation a CP-even Higgs will only be produced if the polarisation direction of the two beams is parallel while for CP-odd states it must be orthogonal. A 3-year run has been simulated running for one year each at maximal linear polarisation with parallel and orthogonal direction and for one year with maximal circular polarisation [11]. Figure 7 (left) shows the mass spectrum for mass-degenerate H,A with linear polarisation. Due to the smaller circular polarisation the background is much higher than in Fig. 6. Figure 7

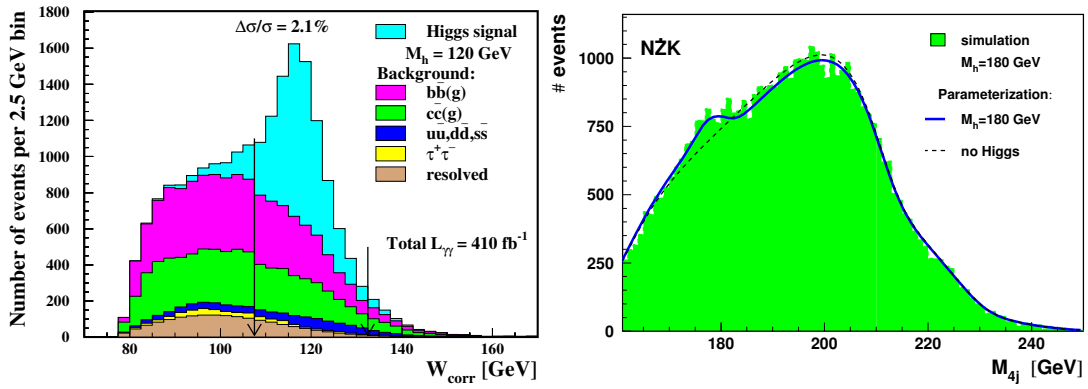

Figure 4: Possible reconstructed mass spectrum for $\gamma\gamma \to H \to b\overline{b}$ (left) [6] and $\gamma\gamma \to H \to WW$ (right) [8].

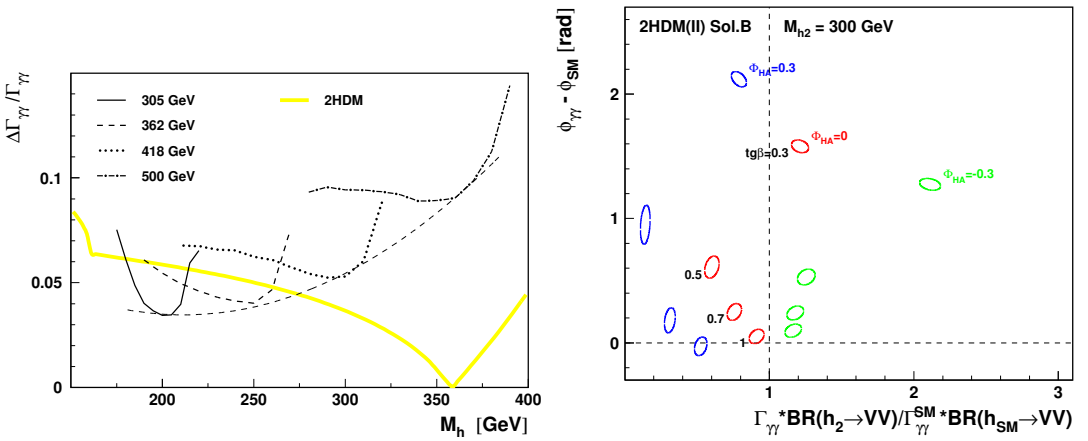

Figure 5: Left: relative precision of $\Gamma_{\gamma\gamma}$ for $H \to WW$ as a function of m_H; right: prediction for the change of $\Gamma_{\gamma\gamma} \times BR(H \to WW)$ and the phase of the coupling for different parameters in a 2HDM model [8].

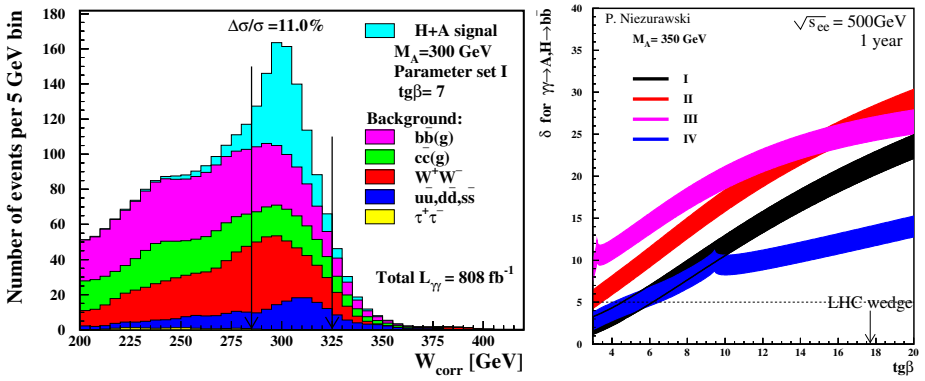

Figure 6: Left: mass spectrum for H, A production at a photon collider; right: H,A discovery range for one year of running at the photon collider. The parameters are defined in [10].

(right) shows the possible cross section measurements for pure CP states. In the case of one pure state, CP can be established with 5σ. If the H and A are mass-degenerate the two cross sections can be measured separately with a 20% precision.

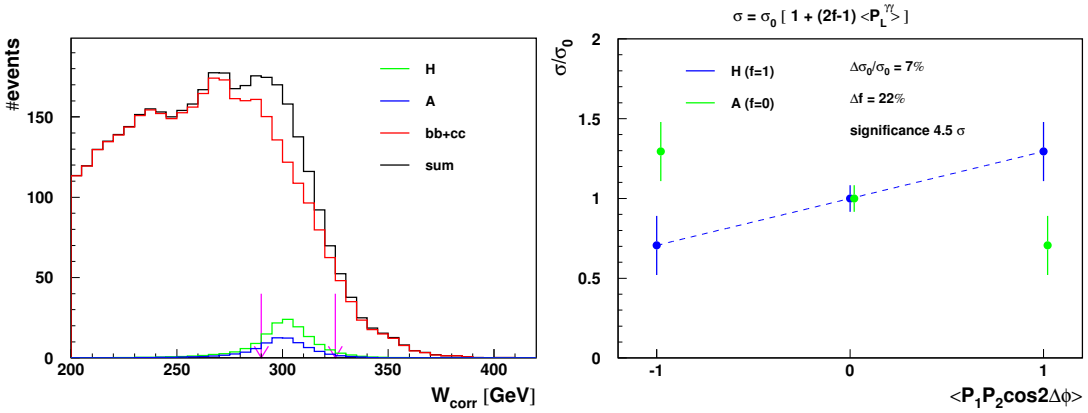

Figure 7: Left: reconstructed mass spectrum for $\gamma\gamma \to H, A \to b\bar{b}$ with linear polarisation; right: possible cross section measurement for $\gamma\gamma \to H \to b\bar{b}$ and $\gamma\gamma \to A \to b\bar{b}$ with one year each on maximal linear polarisation with parallel and orthogonal orientation and one year with zero linear and maximal circular polarisation [11].

The photon collider might also have the possibility to measure $\tan\beta$ [12]. The coupling of the τ to the H and A is proportional to $\tan\beta$ and Higgses can be produced via $\tau\tau$-fusion ($\gamma\gamma \to A\tau^+\tau^-$, $H\tau^+\tau^-$). The cross section is in the fb range (see Fig. 8) so that $\mathcal{O}(100)$ events per year are expected allowing to measure $\tan\beta$ to a few percent [12]. However an experimental study to estimate the reconstruction efficiency and backgrounds is still missing.

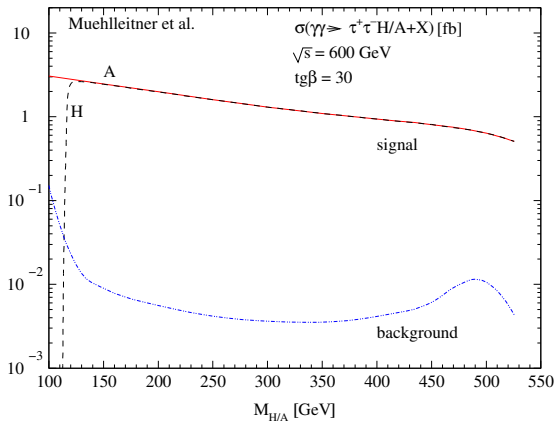

Figure 8: Cross section of the process $\gamma\gamma \to A\tau^+\tau^-$, $H\tau^+\tau^-$ as a function of the A,H mass [12].

3 Supersymmetry

In $\gamma\gamma$ superpartners are produced in pairs so that the reach is somewhat lower than in e^+e^-. However there is a possible discovery window in eγ using the process $e\gamma \to \tilde{e}_r\tilde{\chi}_1^0$. The mass reach for this process is $m(\tilde{e}_r) + m(\tilde{\chi}_1^0) < 0.9\sqrt{s}_{ee}$ which might be larger than the e^+e^- reach for slepton pair production ($0.5\sqrt{s}_{ee}$) if the mass difference $\tilde{e}_r - \tilde{\chi}_1^0$ is large. One needs right handed electrons to produce the $\tilde{e}_r$ which simultaneously reduces the single-W background that otherwise would be huge. An experimental simulation indicates that this channel can indeed be identified at an eγ collider [13]. The resulting mass spectrum is shown in Fig. 9 (left).

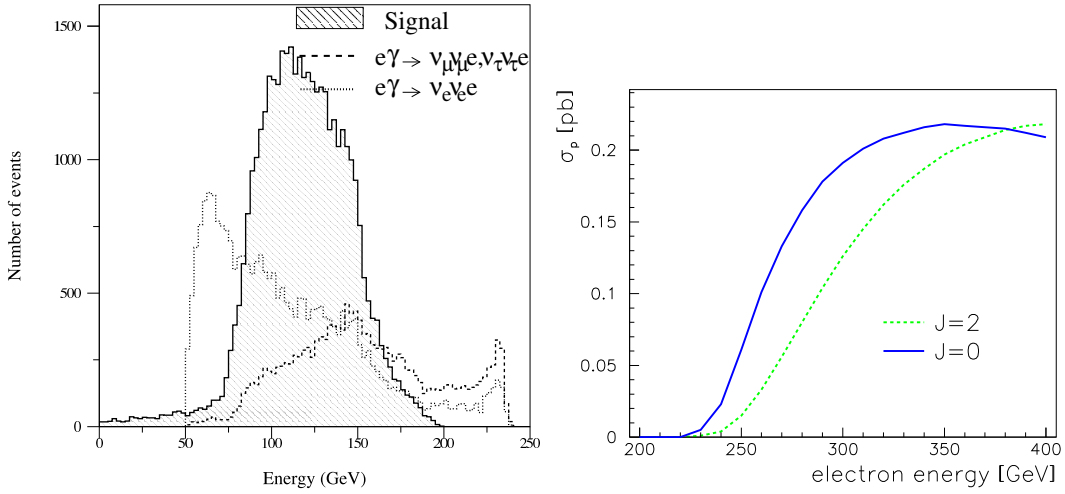

Figure 9: Left: mass spectrum for $e\gamma \to \tilde{e}_r\tilde{\chi}_1^0$ and corresponding backgrounds after cuts [13]; right: effective cross section for $\gamma\gamma \to \tilde{\chi}_1^+\tilde{\chi}_1^-$ for the two beam polarisation sates [14].

In the $\gamma\gamma$-mode all charged superpartners are produced in pairs. The cross sections are large, however the background, typically WW-production, is large as well. The cross sections can be calculated reliably in QED so that the measured event rates are directly proportional to the decay branching ratios. Figure 9 (right) shows the effective cross section[1] of the process $\gamma\gamma \to \tilde{\chi}_1^+\tilde{\chi}_1^- \to W^+W^-\tilde{\chi}_1^0\tilde{\chi}_1^0 \to q\bar{q}q\bar{q}\tilde{\chi}_1^0\tilde{\chi}_1^0$ for a SUSY scenario with $m_{\tilde{\chi}_1^\pm} = 180\,\text{GeV}$, $m_{\tilde{\chi}_1^0} = 96\,\text{GeV}$ and $BR(\tilde{\chi}_1^\pm \to \tilde{\chi}_1^0 W^\pm) = 26\%$ [14]. At $\sqrt{s}_{ee} = 600\,\text{GeV}$ this results in 8000 signal events per year. With an efficiency of 24% and a purity of 11% a measurement of $\frac{\Delta BR(\tilde{\chi}_1^\pm \to \tilde{\chi}_1^0 W)}{BR(\tilde{\chi}_1^\pm \to \tilde{\chi}_1^0 W)} = 3.5\%$ is possible. In the SUSY fits for ILC [15] this result improves the precision of $\tan\beta$ by more than a factor two. However no decay-mode sensitive variables from e^+e^- have been included in the fit up to now.

4 Coupling measurements

The photon-collider is only sensitive to the coupling of charged particles to photons, which has, however, the advantage that there are no ambiguities between the couplings to Z-bosons and photons. The monopole coupling (charge) is given by electromagnetic gauge invariance so that higher order couplings are accessible in the measurements. The best studied case is the γWW couplings which can be measured in $\gamma\gamma \to WW$ and $e\gamma \to \nu_e W$ [16, 17]. The cross section is large ($\sim 80\,\text{pb}$), however there is no sensitivity enhancement due to gauge cancellations. Because of the unknown longitudinal momentum the WW-system can only be fully reconstructed if both W-bosons decay hadronically. However, with symmetric beams the polar angle ambiguity $\theta \leftrightarrow \pi - \theta$, that arises because the W-charge cannot be measured, does not matter. In the $\gamma\gamma$-mode both polarisation states are sensitive to the triple gauge couplings. The J=0 state is, however, problematic since the luminosity cannot be measured accurately. Figure 10 compares the sensitivities to κ_γ and λ_γ at the different machines. For κ_γ, which is the more interesting coupling because of the lower mass dimension, the e^+e^--mode of the ILC is the by far most sensitive possibility. For λ_γ the $\gamma\gamma$ and $e\gamma$ modes are more sensitive than e^+e^-, however the LHC has a similar potential.

5 Conclusions

Depending on the physics scenario the photon collider can be an important addition to the e^+e^--mode of the ILC. For the interpretation of the data from the photon collider and for the final decision if the photon collider should be built data from e^+e^- are needed, so the the $\gamma\gamma$ mode should run after e^+e^-. This is also technically the preferred solution because the photon collider is more challenging with respect to the beam parameters and more difficult to set up. To exploit fully the physics case of the photon collider also the highest possible beam energy is needed.

For these reasons it is important that the design of the ILC includes the photon collider as an option that can run with maximum luminosity after or interleaved with the e^+e^- mode.

[1] The effective cross section is obtained by folding the $\gamma\gamma \to \tilde{\chi}_1^+\tilde{\chi}_1^-$ cross section with the luminosity spectrum.

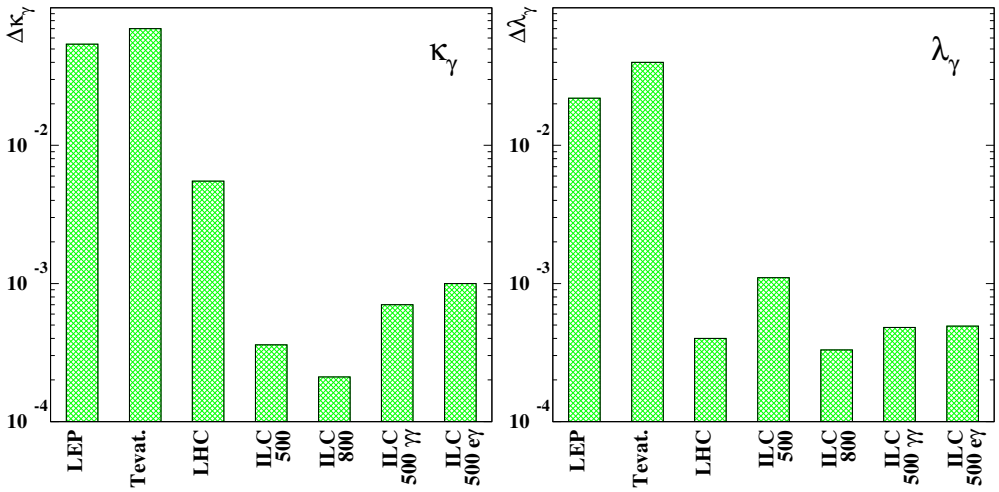

Figure 10: Sensitivity to κ_γ and λ_γ at the different machines [3].

References

[1] I. F. Ginzburg, G. L. Kotkin, V. G. Serbo, and V. I. Telnov *JETP Lett.* **34** (1981) 491–495.

[2] ECFA/DESY Photon Collider Working Group , B. Badelek *et al.*, "TESLA Technical Design Report, Part VI, Chapter 1: Photon collider at TESLA.". DESY-01-011E.

[3] F. Bechtel *et al. Nucl. Instrum. Meth.* **A564** (2006) 243–261, `arXiv:physics/0601204`.

[4] P. Chenand, T. Ohgaki, T. Takahashi, A. Spitkovsky, and K. Yokoya *Nucl.Instr.Meth.* **A397** (1997) 458–464.

[5] A. Djouadi *et al.* `arXiv:0709.1893 [hep-ph]`.

[6] P. Niezurawski `arXiv:hep-ph/0507004`.

[7] K. Monig and A. Rosca *Eur. Phys. J.* **C57** (2008) 535–540, `arXiv:0705.1259 [hep-ph]`.

[8] P. Niezurawski, A. F. Zarnecki, and M. Krawczyk `arXiv:hep-ph/0307175`.

[9] ATLAS Collaboration, Physics TDR, CERN-LHCC-99-14 and CERN-LHCC-99-15.

[10] P. Niezurawski, A. F. Zarnecki, and M. Krawczyk *Acta Phys. Polon.* **B37** (2006) 1187–1191.

[11] A. F. Zarnecki, P. Niezurawski, and M. Krawczyk `arXiv:0710.3843 [hep-ph]`.

[12] S. Y. Choi *et al. Phys. Lett.* **B606** (2005) 164–172, `arXiv:hep-ph/0404119`.

[13] I. Alvarez Illan and K. Mönig, "Selectron production in $e\gamma$ collisions at a linear collider.". LC-PHSM-2005-002.

[14] G. Klamke and K. Moenig *Eur. Phys. J.* **C42** (2005) 261, `arXiv:hep-ph/0503191`.

[15] P. Bechtle, K. Desch, W. Porod, and P. Wienemann `hep-ph/0511006`.

[16] K. Mönig and J. Sekaric *Eur. Phys. J.* **C38** (2005) 427–436, `hep-ex/0410011`.

[17] K. Mönig and J. Sekaric `hep-ex/0507050`.